Sloshing and Violent in-Chamber Water Column Movement in an OWC Wave Energy Converter

Krisna Adi Pawitan[#1], William Allsop[#2], Tom Bruce[#3]

[#]*Institute for Energy Systems (IES), University of Edinburgh*
King's Buildings, Edinburgh EH9 3JL, United Kingdom

[1]K.Pawitan@ed.ac.uk,

[2]W.Allsop@ed.ac.uk

[3]Tom.Bruce@ed.ac.uk

***Abstract*— The development of oscillating water column (OWC) wave energy converter (WEC) has been very extensive in the last couple of decades with the successful grid connection of the European pilot projects such as, LIMPET, OWC Pico power plant, and Mutriku wave energy plant. The water column behaviour in the OWC chamber, however, usually assumed to be well behaved during operation in the design process. This assumption later proven to be not accurate with damaged received inside the caisson chamber, most likely due to chamber sloshing. This paper aims to observe the water column behaviour during various type of wave condition for both regular and irregular wave settings. The experiment involves a small-scale physical model, pressure transducer, and wave gauges in the University of Edinburgh long wave flume facility. The results show that sloshing is more likely to occur in the longer wave length relative to the chamber width, higher wave height, and less chamber pressure generated. Four types of water column behaviours (well behaved/no sloshing, low sloshing, medium sloshing, and high sloshing) was characterised. A ceiling impacts up to at least 1.25ρgH was observed during sloshing.**

***Keywords*— wave energy converter, oscillating water column, marine renewable, chamber sloshing, sloshing characterisation**

I. INTRODUCTION

The development of wave energy converter has been very extensive in the last couple of decades. The concept of using wave as an energy generation device dated back to 1940s with main purpose of powering a navigation buoy, designed by Yoshio Matsuda, as mentioned in [1]. This device utilised an oscillating water column (OWC) inside a floating buoy to rotate a conventional unidirectional air turbine. Although many types of wave power energy generator mechanism explored since then, the OWC type mechanism excel in terms of simplicity and low maintenance cost. The energy generator uses the water column to push and suck air out of and into the chamber through the power take-off (PTO) mechanism. This allows minimum chance of the PTO system to touch the water, avoiding the possibility of corrosion and biofouling due to seawater.

Several European pilot projects for the OWC typed wave energy converter (WEC) devices, such as LIMPET [2], OWC Pico power plant [3], and Mutriku wave energy plant [4], managed to successfully connect to the national electricity grid over the last 20 years. Although LIMPET operated below the design capacity, even during peak performance, it managed to operate over 90% of the time before finally decommissioned [5,6]. This proves, however, that the OWC type wave energy converter can generate electricity reliably. The other pilot projects, OWC Pico power plant and Mutriku wave energy plant, haven't been a smooth success as well. Pico power plant has been closed due to partial structure failure after fulfilled its purpose as a pilot demonstration project for OWC-WEC in Europe [7]. Mutriku wave power plant, on the other hand, received severe damaged during construction due to extreme weather [8]. Fortunately, the wave power plant is still able to operate until now after it was fixed and commissioned in July 2011. LIMPET poor efficiency and both Pico and Mutriku structural problems, emphasise the importance of further exploration in the OWC wave loading and water column behaviour uncertainties.

Most of the time, during the design stage, the water column inside the OWC chamber is assumed to behave well with calm water surface during operation. Latest experiment, however, shows that it is not always the case. During a certain sea condition, the research shows that the water column inside LIMPET power station OWC chamber became chaotic and far from the calm and well-behaved assumption [9]. This water column movement is called sloshing. In the more extreme cases, the sloshing movement may cause slam(s) on the ceiling of the chamber. Further Particle Imaging Velocimetry (PIV) experiment on the water column inside the chamber found a vortex was formed just behind the front wall when the incident wave passed, especially in the low value in-chamber damping coefficient condition [10].

These recent findings highlighted the uncertainty and unpredictability of the water column behaviour and wave loading inside the chamber for an oscillating water column wave energy converter design. The ability of predicting such sloshing and more violent motion inside the OWC chamber during operation could be crucial for the survivability of the structure and the efficiency of the wave energy converter device. Sloshing phenomenon is not uncommon and should be part of the design consideration. This paper aims to characterise the wave condition under which the violent sloshing water column occurs for both regular and irregular wave conditions.

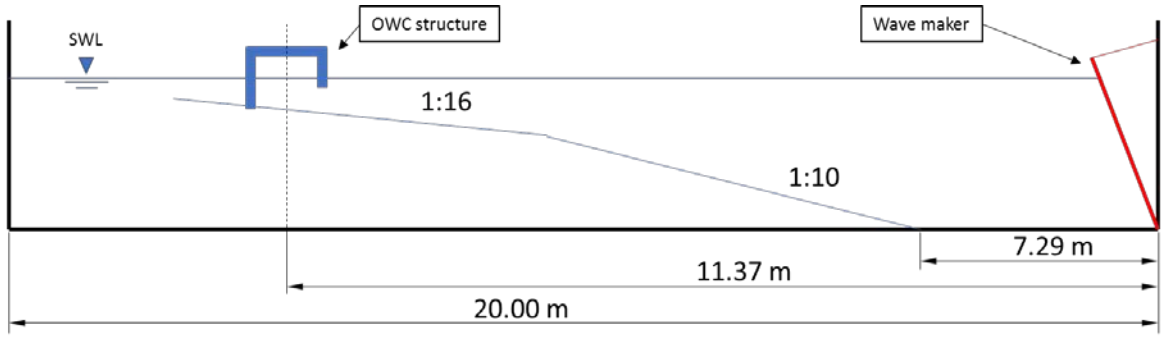

Figure 1 Schematics of the long wave flume and the model structure location with dimension shown in metre.

II. METHODOLOGY

In order to observe the water column behaviour of an OWC chamber during operation, a small-scale physical model measurement of an Oscillation Water Column (OWC) installed in a vertical breakwater is done. The model's geometry is loosely based upon the structure of Mutriku wave power plant located in Basque Country, Spain [4], and the then-proposed device in Siadar, Scotland [11]. The experiment was done in the University of Edinburgh long wave flume facility as schematics' shown in Figure 1. The flume is 20 m long and equipped with an absorption vane installed on the very end of the flume. The waves are generated using a flap-type wave make with good absorption capability based on feed back control. The small-scale physical model is placed 11.37 m from the wave generator. There were slopes located in front of the wave generator leading to the model structure. The foreshore was made using two 3-m long boards made of plastic. The foreshore slope included an elbow from a 1:10 to a 1:16 gradient. The wave paddle is capable of producing wave heights of up to 0.12 m, and wave periods in the range of 0.5s to 3s. The full water depth used during the experiment is 0.7 m, which fell in the transitional wave according to Airy theory.

The model OWC (Figure 2) utilised a pressure transducer located at the centre of the ceiling to record the chamber pressure and any wave loads acting on the ceiling of the chamber. The physical model height is 290 mm height, 285 mm wide, and 280 mm long. The in-chamber dimension, however, is 250 mm height, 285 mm wide, and 260 mm long. There is a gap of approximately 40 mm between the ceiling of the chamber and the top of the physical model structure for structural stability of the physical model. Figure 3 shows the detailed cross-sectional dimensions of the OWC chamber inside the structure in mm and the location of the pressure transducer used (indicated by the solid red diamond). The model has an interchangeable orifice opening located in the centre of the ceiling. This configuration allows the orifice diameter to be changed during the experiment.

The orifice opening is used to simulate the power take-off resistance (PTO). The smaller orifice opening represents higher power take-off resistance. The experiments utilised 8 different orifice diameter, consist of a closed orifice to simulate a closed chamber condition and several open orifices

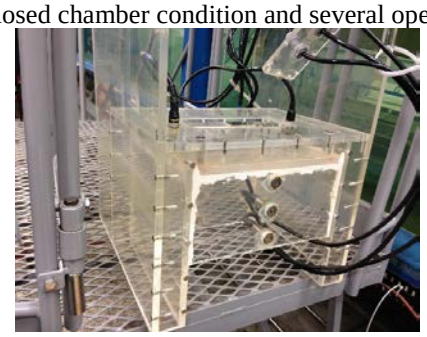

Figure 2 Image of the physical model used in the experiment.

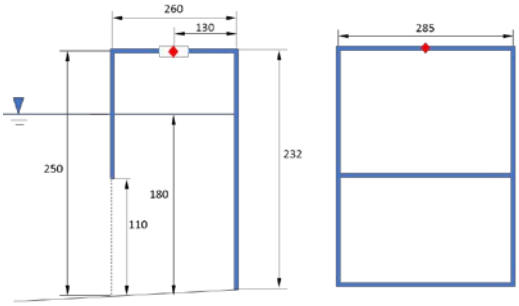

Figure 3 The cross-sectional image of the physical model used with detailed dimension of the chamber in mm. Solid red diamond shows the position of the pressure transducer used.

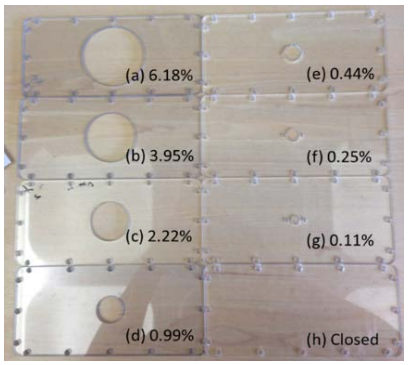

Figure 4 Various orifice openings used for the experiment with orifice:chamber area ratio of (a) 6.18%, (b) 3.95%, (c) 2.22%, (d) 0.99%, (e) 0.44%, (f) 0.25%, (g) 0.11%, and (h) Closed (0.0%).

to simulate the operating and fully open chamber conditions. For simplification, the chamber opening will be presented as the orifice:chamber area ratio (A_o/A_c). Figure 4 shows the range of orifices used during the experiment with: (a) 6.18%, (b) 3.95%, (c) 2.22%, (d) 0.99%, (e) 0.44%, (f) 0.25%, (g) 0.11%, and (h) closed orifice (0.00%). It should be noted that the use of an orifice to simulate PTO resistance is more representative of an impulse turbine then a wells turbine.

In addition to the pressure transducer and the orifice opening, the experiment also utilised 7 wave gauges to measure the water elevation in 7 different locations. The wave gauges used were the Edinburgh Designs resistance-type wave gauge. A set of three wave gauges was installed in the shallower part of the flume and in front of the structure. Another set of three wave gauges was installed in the deeper part of the flume near the wave generator. One wave gauge was installed inside the chamber through the opening orifice to measure the water column elevation during the experiment, with the exception of the closed orifice condition test. An additional test with only the slopes installed and without the structure was done in order to measure the incident wave without any reflection from the structure, although a small degree of reflection from the slope is still exists. The two sets of three wave gauges are installed according to Mansard and Funke's three probe reflection analysis [12].

The regular waves are recorded in the frequency of 2000 Hz and the irregular wave in the range frequency of 500Hz to 1000Hz depending on the duration of the recording. The regular waves were recorded in the duration of 90 seconds, while the irregular waves were recorded for at least 1000 wave cycles. The irregular wave was generated based on JONSWAP spectra with peak enhancement factor (γ) of 3.3. The experiment was recorded using a video camera which located outside of the wave fume and recorded the water column in the OWC chamber through the flume side wall (glass) and the chamber structure wall (perspex). The see-through material of both the wave flume side wall and the physical model allows the water column to be observed from the recording location.

III. Result and Discussion

A. *Sloshing Characterisation*

Before discussing the sloshing regime of the sloshing, this sub-section explores the definition of the observed intensity of sloshing. The intensity is qualitatively observed based on the surface water column movement and oscillation behaviour during the experiment. Figure 5 shows the different of chamber water level behaviour between the well behaved condition (blue) and sloshing condition (orange). As can be seen the water column movement is not oscillating smoothly under sloshing condition. Figure 6 (a) and (b) show an example of the no sloshing where the water column surface is calm and well behaved during oscillation (solid red line). Figure 7 (a) and (b) demonstrate the low sloshing characteristics where the water surface is not calm, but the vertical oscillation is still clearly visible, and no impacts are observed during the event.

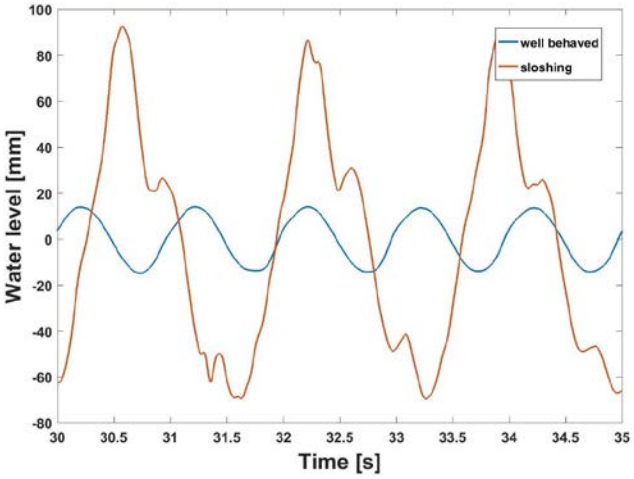

Figure 5 In-chamber water column movement for the well behaved (blue) and sloshing (orange) conditions in mm.

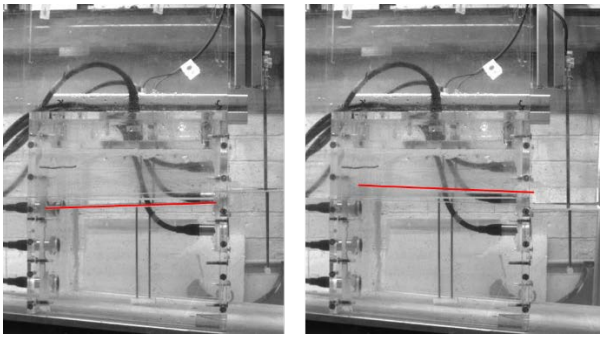

Figure 6 Well behaved (no sloshing) water column behaviour with solid red line showing the water surface

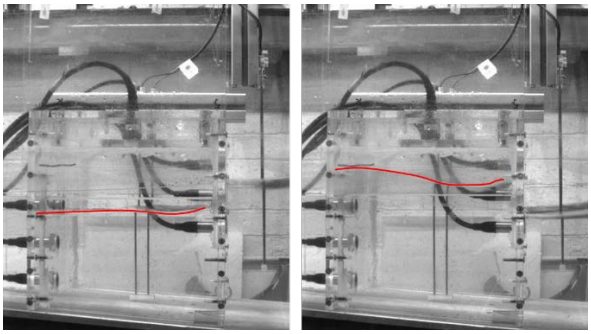

Figure 7 Low sloshing water column behaviour with solid red line showing the water surface

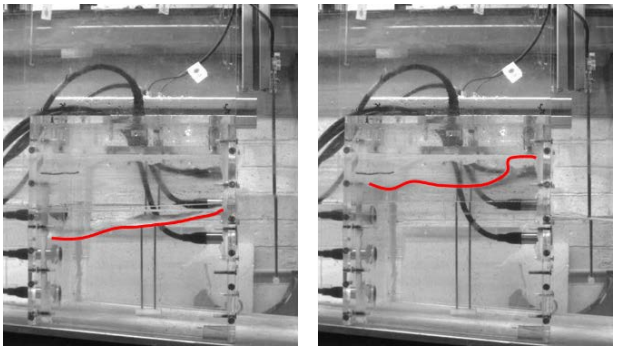

Figure 8 Medium sloshing water column behaviour with solid red line showing the water surface

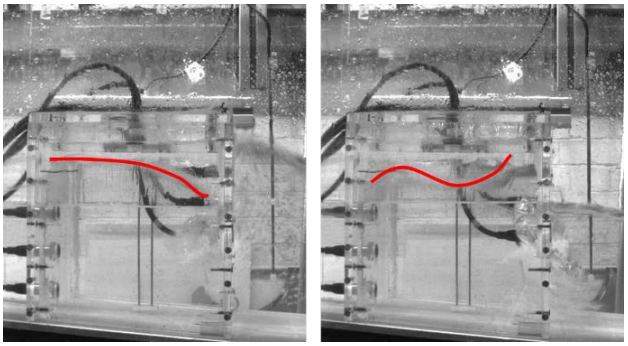

Figure 9 High sloshing water column behaviour with solid red line showing the water surface

Figure 8 (a) and (b) show a medium sloshing condition where the water surface shows a significant difference between the front part of the chamber and the rear part of the chamber, with a minor impact on the ceiling observed in (b). Figure 9 (a) and (b) show a high sloshing condition with chaotic water column surface and clear impact or slam(s) observed on the ceiling of the chamber. The water column movement can be described as follow: the water near the rear of the chamber rises until it reaches the ceiling more or less coincident with the arrival of the subsequent incident wave crest at the front face (a). The wave is later reflected by the rear wall and flows to the front part of the chamber, rises up the front wall, and hits the front part of the chamber (b).

For simplification, the water column behaviour is characterised using colour codes based on the intensity with green denoting well behaved / no sloshing, blue denoting low sloshing, yellow denoting medium sloshing, and red denoting high sloshing. The characterisation was done for both regular wave condition (sub-section *A*) and irregular wave condition (sub-section *B*).

Several symbols are also used to describe the condition of the chamber water column, such as: wave overtopping (*), water column oscillation reaches the ceiling of the chamber (^). During the wave overtopping event, sometimes the water poured back into the chamber from the orifice opening and increase the still water level inside the chamber. This condition is denoted with (Π). An additional symbol is also used to describe the wave condition that is not tested (-).

A. *Regular wave sloshing regime*

TABLE I

SLOSHING REGIME FOR REGULAR WAVE CONDITION AT VARIOUS CHAMBER WIDTH CHARACTERISTICS (B_c/L), WAVE HEIGHT (H), AND ORIFICE:CHAMBER AREA RATIO (A_o/A_c) AND ADDITIONAL SYMBOL FOR WAVE OVERTOPPING (*), WAVE OVERTOPPING FOLLOWED BY CHAMBER WATER LEVEL RISE (Π), WATER COLUMN OSCILLATION REACHES THE CEILING OF THE CHAMBER (^), AND NOT TESTED (-).

Bc/L	H (m)	Orifice opening:chamber area ratio (A_o/A_c)							
		(closed)	0.11%	0.25%	0.44%	0.99%	2.22%	3.95%	6.18%
0.165	0.02	-	-	-	-				
	0.03								
	0.04								
	0.06								
	0.07								
	0.09								
0.099	0.02	-	-	-	-				
	0.05								
	0.07								
	0.09								
	0.11	*	* Π	* ^	*			-	
0.070	0.08								^
	0.09								
	0.12	*	*Π	*Π	*Π				
0.055	0.02	-	-	-	-				
	0.04								
	0.08							^	^
	0.11	*	*Π	*Π	*Π				^

Table 1 shows the observation result of the sloshing regime for the regular wave condition test. The regime is separated based upon the chamber width characteristics (B_c/L), wave height (H), and opening:chamber area ratio (A_o/A_c). The sloshing appears to most likely occurs if the wave height is relatively high. Furthermore, it is more likely to slosh if the chamber width is relatively shorter than the wave length. It is consistent across different relative chamber widths and wave heights that the sloshing occurs on the bigger orifice:chamber area ratio. This is as anticipated due to lack of chamber pressure generated during the operation. Figure 10 (a) shows the chamber pressure measured during the experiment for B_c/L = 0.165 and H = 0.09 m (solid blue circle) and B_c/L = 0.07 and H = 0.09m (solid orange circle). Figure 10 (b) (solid lines) shows the sloshing status of the corresponding colour data points. The chamber pressure in (a) can be divided into two zones: no to low sloshing zone and the medium to high sloshing zone based on the sloshing status in (b). As the figure demonstrated, the medium to high sloshing tend to occur on the less chamber pressure generation. Noted that the orange coloured data has higher degree of sloshing compare to the blue coloured data almost on all of the orifice:chamber area ratio. This support the analysis that sloshing is more likely to happen in a longer wave length for the same chamber width.

Apart of the negative affect of sloshing to the performance of the wave energy converter, a sloshing impact on the ceiling of the chamber during high sloshing event can also be observed. A pressure transducer was utilised in the centre of the ceiling (on the side of the orifice opening) to measure the impact on the chamber ceiling. The pressure measurement of B_c/l = 0.055 and H = 0.11 m is shown in Figure 11 in solid black line with the corresponding y-axis on the left side showing the measured ceiling pressure. The water level measurement inside the chamber is presented in the same graph in solid orange with the corresponding y-axis on the right side showing the water elevation in mm. Both data is shown in the same time step in x-axis. The graph shows that the impact loads on the centre of the ceiling could reach up to 1354 Pa (1.25ρgH). Unfortunately, as can be seen in Figure 9, the impact also occurs on the rear part of the chamber ceiling followed by another impact to the front part of the ceiling. Having the pressure transducer in the centre of the ceiling, means that the complete impact on the ceiling is not captured. It is therefore likely that the maximum impact on the rear and the front part of the ceiling is higher than the one recorded in the centre.

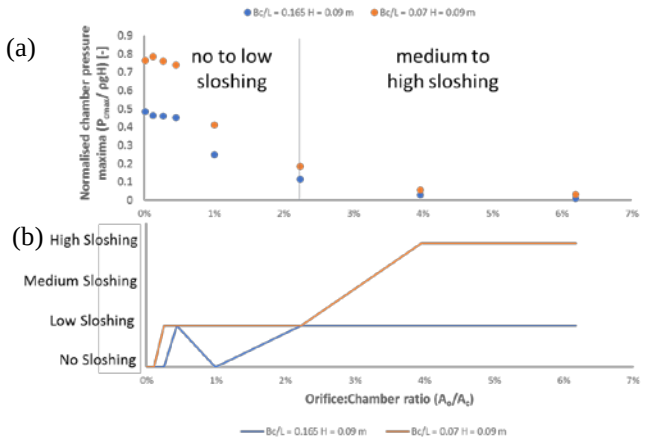

Figure 10 (a) Chamber pressure maxima measurement for B_c/L = 0.165 H = 0.09 m (blue circle) and B_c/L = 0.07 H = 0.09 m (orange circle) vs orifice:chamber area ratio; (b) sloshing status for the same colour data points vs orifice:chamber area ratio

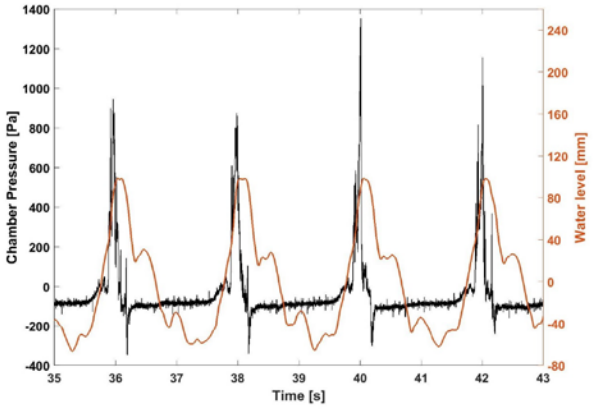

Figure 11 Time history chamber pressure measurement on the chamber ceiling (left y-axis, black) and chamber water column elevation (right y-axis, orange) at the same time step.

B. *Irregular wave sloshing regime*

Unlike the regular wave condition, the wave height and wave period changes between each wave cycle for the irregular wave condition. Due to this condition the sloshing event might occurs in a single wave cycle and then disappear in the next one. The sloshing status is then based on the observation if the sloshing event occurs even only once during the entire experiment An additional symbol for venting (v) is also used in the figure. Venting is a phenomenon where the water level fell below the lower edge of front wall and allows the outer air to enter the chamber as demonstrated in Figure 12. The red arrow shows the movement of the air entered into the chamber through the front wall opening. This condition effects the negative pressure generated inside the chamber by the trough of the wave and allows the chamber pressure to return toward the atmospheric pressure via the front wall opening instead of the power take-off. Figure 13 shows the chamber pressure measurement of the closed orifice, B_c/L = 0.0991, and H_{m0} = 0.069m during the venting phenomenon in Figure 12. Since it is a closed chamber condition, the pressure

TABLE II

SLOSHING REGIME FOR IRREGULAR WAVE CONDITION AT VARIOUS CHAMBER WIDTH CHARACTERISTICS (B_c/L), SIGNIFICANT WAVE HEIGHT (H_{m0}), AND ORIFICE:CHAMBER AREA RATIO (A_o/A_c) AND ADDITIONAL SYMBOL FOR WAVE OVERTOPPING (*), WAVE OVERTOPPING FOLLOWED BY CHAMBER WATER LEVEL RISE (Π), WATER COLUMN OSCILLATION REACHES THE CEILING OF THE CHAMBER (^),NOT TESTED (-), AND VENTING (V).

Bc/L	H_{m0}	Orifice opening:chamber area ratio (A_o/A_c)							
		closed	0.11%	0.25%	0.44%	0.99%	2.22%	3.95%	6.18%
0.1650	0.030						-	-	-
	0.045	-					-	-	-
	0.059	*	*	*	*				
0.0991	0.046	*	*		*		-	-	-
	0.069	V	v*	*	*	*	^ *	^	^
0.0702	0.062	*	*	*		*	^*	^	^
0.0547	0.077	V	v*	v*	*Π	^*	^*	^*	^*
0.0823	0.030	-				-	-	-	-

generated (both negative and positive) reflects the maximum idealised chamber pressure generated. The zero value in the graph represents the atmospheric pressure. As can be seen from the figure, the average pressure increases above the atmospheric pressure and generate less negative pressure after venting. One can image that such phenomenon could affect the negative pressure generated during the operation. Table 2 shows the observation result for the irregular wave condition. The figure used same characteristics chamber width (B_c/L) and orifice:chamber area ratio (A_o/A_c) as the regular wave observation. The wave height shown, however, is the significant wave height (H_{m0}) of the irregular wave condition. The water column seems to be more likely to slosh during irregular wave conditions. The same trend of sloshing occurrence in the longer wave conditions and higher wave heights seems to be in line with the regular wave condition. Venting phenomenon ("v" symbol) tends to occur on the closed and smaller orifice:chamber area ratio, and disappear on the larger ratio. The water column is more likely to touch the ceiling of the chamber in the larger orifice:chamber area ratio, which makes sense due to lack of chamber pressure generated. Wave overtopping (*) is also more likely to occur during closed and smaller opening ratio and the occurrence is reduced in the larger opening ratio.

IV. CONCLUSIONS

A series of experiments to observe the water column behaviour of an Oscillating Water Column (OWC) integrated in a vertical breakwater is done for both regular and irregular wave conditions. The results show that sloshing is not uncommon for both regular and irregular wave conditions. The water column behaviour is characterised into well behaved (no sloshing), low sloshing, medium sloshing, and high sloshing conditions. The water column behaviour is characterised based on the characteristics chamber width

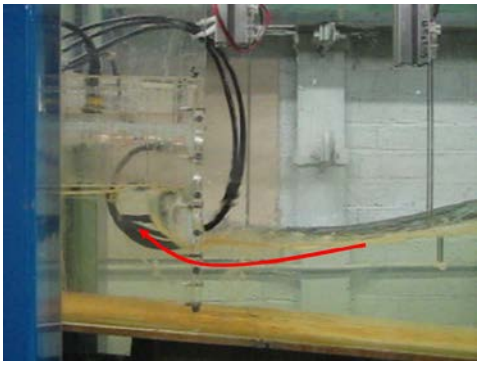

Figure 12 Venting phenomenon where the water level fell below the chamber opening and air enters the chamber through the front opening indicated by the solid red arrow.

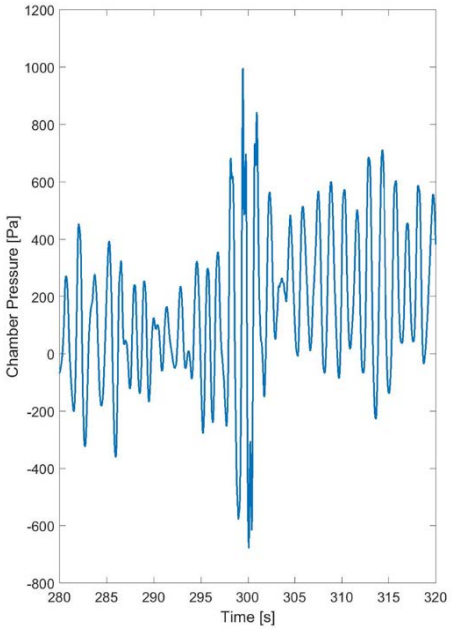

Figure 13 Time history chamber pressure measurement during the venting event.

(B_c/L), wave height (H) or significant wave height (H_{m0}), and the orifice opening:chamber area ratio (A_o/A_c). It can be concluded that sloshing is more likely to occurs on the longer wave length relative to the chamber width, higher wave height, and less chamber pressure generated. Venting phenomenon was also observed during the irregular wave condition and this allows the negative pressure generated by the wave trough to be reduced. Both wave-overtopping and venting phenomena are more likely to be observed in the closed and smaller orifice:chamber area ratio and reduced in the larger orifice:chamber area ratio. Observation in both the regular and irregular waves support this argument. The sloshing impact acting on the centre of the ceiling has been successfully quantified, although the maximum impact pressure due to sloshing event is more likely to occur on the rear and front part of the chamber ceiling.

ACKNOWLEDGMENT

The first author would like to thank to the Indonesia Endowment Fund for Education (LPDP) for the financial support for his studies in the University of Edinburgh and enables this study to be carried out.

REFERENCES

[1] Falcão, A. F., & Henriques, J. C. (2016). Oscillating-water-column wave energy converters and air turbines: A review. *Renewable Energy*, *85*, 1391-1424.

[2] Boake, C. B., Whittaker, T. J., Folley, M., & Ellen, H. (2002, January). Overview and initial operational experience of the LIMPET wave energy plant. In *The Twelfth International Offshore and Polar Engineering Conference*. International Society of Offshore and Polar Engineers.

[3] Pecher, A., Kofoed, J. P., Le Crom, I., Neumann, F., & Azevedo, E. D. B. (2011, January). Performance assessment of the Pico OWC power plant following the EquiMar Methodology. In *The Twenty-first International Offshore and Polar Engineering Conference*. International Society of Offshore and Polar Engineers.

[4] Torre-Enciso, Y., Ortubia, I., de Aguileta, L. L., & Marqués, J. (2009, September). Mutriku wave power plant: from the thinking out to the reality. In *Proceedings of the 8th European Wave and Tidal Energy Conference, Uppsala, Sweden* (Vol. 710).

[5] Islay LIMPET Wave Power Plant, The Queen's University of Belfast Contract JOR3-CT98-0312 Publishable Rep., 1 November 1998 to 30 April 2002, [Online], Available: http://mhk.pnnl.gov/wiki/images/2/25/Islay_LIMPET_Report.pdf.

[6] Whittaker, T. J. T., Beattie, W., Folley, M., Boake, C., Wright, A., Osterried, M., & Heath, T. (2004). The Limpet Wave Power Project–the first years of operation. *Renewable Energy*.

[7] Brito-Melo, A. (2018) Press release Wave Pico Plant [Online]. Available: http://www.pico-owc.net/news.php?cat=89&newid=346&wnsid=ffaedab643e41be91f9eecf88f429ee8.

[8] Medina-Lopez, E., Allsop, N. W. H., Dimakopoulos, A., & Bruce, T. (2015). Conjectures on the Failure of the OWC Breakwater at Mutriku. In *Proceedings of Coastal Structures and Solutions to Coastal Disasters Joint Conference, Boston, Massachusetts*.

[9] Müller, G., & Whittaker, T. J. (1995). Visualisation of flow conditions inside a shoreline wave power-station. *Ocean engineering*, *22*(6), 629-641.

[10] López, I., Castro, A., & Iglesias, G. (2015). Hydrodynamic performance of an oscillating water column wave energy converter by means of particle imaging velocimetry. *Energy*, *83*, 89-103.

[11] Patterson, C., Dunsire, R., & Hillier, S. (2010). Development of wave energy breakwater at Siadar, Isle of Lewis. In *Coasts, marine structures and breakwaters: Adapting to change: Proceedings of the 9th international conference organised by the Institution of Civil Engineers and held in Edinburgh on 16 to 18 September 2009* (pp. 1-738). Thomas Telford Ltd.

[12] Mansard, E. P., & Funke, E. R. (1980). The measurement of incident and reflected spectra using a least squares method. In *Coastal Engineering 1980* (pp. 154-172).